



## Electrodeposition of Nano Hydroxyapatite Coating on Biodegradable Mg-Zn Scaffold

Z. S. Seyedraoufi\*, S. Mirdamadi, S. Rastegari

Center of Excellence for High Strength Alloys Technology (CEHSAT), School of Metallurgy and Materials Engineering, Iran University of Science and Technology, 16846-13114, Tehran, Iran

### PAPER INFO

#### Paper history:

Received 11 September 2013

Received in revised form 17 October 2013

Accepted 12 December 2013

#### Keywords:

Biodegradable Mg-Zn Scaffold

Nano Hydroxyapatite Coating

Electrodeposition

Corrosion Resistance

### ABSTRACT

In this research, porous magnesium-zinc scaffolds were prepared by powder metallurgical process and nano hydroxyapatite (HAP) coating on the Mg-3Zn (wt.%) scaffold was prepared by pulse electrodeposition and alkali treatment processes to improve the corrosion resistance of the scaffold. The results indicated the as-deposited coating consists of HAP, DCPD and OCP with needle-like and plate-like structures and the post-treated coating was composed of needle-like particles of nano HAP that developed almost perpendicularly to the substrate. Electrochemical tests showed that the corrosion potential of scaffold significantly increased from -1.475 to -1.365 V and the corrosion current density reduced 1.5-fold in comparison to the scaffold modified by nano hydroxyapatite coating.

doi: 10.5829/idosi.ije.2014.27.06c.12

## 1. INTRODUCTION

There has been an increasing interest in porous scaffold substitutes for bone tissue engineering applications because osteoblasts obtained from the patient's hard tissues can be expanded in culture and seeded onto the scaffold that will be gradually integrated with new bone tissues [1, 2]. Magnesium has been recognised as a very promising biomaterial for bone implants in load-bearing applications because of its excellent mechanical properties, low density and biodegradability [1-5]. The high corrosion rate of Mg alloys leads to high concentrations of Mg ion and hydrogen gas release, thus, control of Mg and Mg alloys corrosion rate is essential [6-8].

In order to improve the corrosion resistance of magnesium alloys, effective approaches might be the application of alloying elements such as Zn and surface modified with hydroxyapatite (HA). HA is currently used as a biomedical material due to its excellent biocompatibility and bioactivity [9]. Nano HAP coating can have structure that is more matched to the bone structure in which the implants should function and

have lower sintering temperature. Many processes have been created to synthesis of HA coatings on metallic substrates, such as biomimetic, sol-gel, electrophoretic deposition, sputtering processes; but, because Mg and Mg alloys have low melting point, these methods cannot be used to deposit HA coating [10]. Electrochemical deposition has unique advantages due to its capability of forming a uniform coating on a porous substrate or one with a complex shape, its controllability with regard to the thickness and chemical composition of the coating, and its low deposition temperature [9-11]. Also, by changing of the electrochemical potential and electrolyte concentration, the morphology of coating can be controlled [10]. In the traditional electrodeposition process, loose, porous and low adhesive coatings develop. Thus, in order to solve this problem, pulse electrodeposition method is suggested for deposition of an adherent coating [8-14]. Because corrosion resistance of Mg-Zn alloy can be reduced by Zn of more than 3% [7], we synthesized Mg-3Zn (wt.%) scaffold as substrate. Porous Mg-3Zn (wt.%) specimens have been prepared using a powder metallurgy method; then, HA coating was deposited on the porous Mg-3Zn (wt.%) scaffold using the pulse electrochemical deposition method and post-treated in alkali solutions. The microstructural and compositional changes of HA

\*Corresponding Author Email: [zahraseyedraoufi@iust.ac.ir](mailto:zahraseyedraoufi@iust.ac.ir) (Z. S. Seyedraoufi)

coating after post-treatment, as well as the degradation behavior of as-synthesized, as-deposited and post-treated porous Mg-3Zn (wt.%) samples in simulated body fluid (SBF) were investigated.

## 2. EXPERIMENTAL PROCEDURE

**2. 1. Synthesis of Scaffold** Pure Mg (purity  $\geq 99\%$ , particle size  $\leq 100\mu\text{m}$ ) and pure Zn (purity  $\geq 99.8\%$ , particle size  $\leq 45\mu\text{m}$ ) powders purchased from Merck were utilised as starting materials. Urea ( $\text{CO}(\text{NH}_2)_2$ ) particles purchased from Merck with a purity of 99.9% were employed as the space-holder. The particle size of the spacer agent material was in the range of 200-400 $\mu\text{m}$ . After mixing the starting materials with the space-holder particles, porous Mg-3Zn (wt.%) samples were prepared via a powder metallurgy method. The mixtures of Magnesium and Zinc powder were prepared based on 3 weight percent zinc, while the urea particles were thoroughly added to the above specimens with volume content of 15%.

The mixed powder was uniaxially pressed at a pressure of 200MPa into green compacts 10 mm in diameter and 10 mm in length. The green compacts were then heat treated to burn out the spacer particles, and to sinter into the porous Mg Scaffolds in a tube furnace under an argon atmosphere. The heat-treatment process consists of two steps, i.e. at 250°C for 4h and 550°C for 2h.

**2. 2. Synthesis of HA Coating** The synthesized Mg-3Zn (wt.%) scaffold was considered as the substrate material. During the electrodeposition, Mg-3Zn (wt.%) scaffold was used as the working electrode and a cylindrical graphite served as the counter electrode. Before deposition, the samples were sequentially polished with silicon carbide papers of 400–1000 grits, cleaned ultrasonically in acetone, activated with 10%  $\text{HNO}_3$  for 10 seconds, and dried using a drying apparatus. The electrolyte used for deposition of calcium phosphate was prepared by mixing a solution of 0.042mol.L<sup>-1</sup>  $\text{Ca}(\text{NO}_3)_2$ , 0.025mol.L<sup>-1</sup>  $\text{NH}_4\text{H}_2\text{PO}_4$  and 0.1mol.L<sup>-1</sup>  $\text{NaNO}_3$ . The pH value of the electrolyte was adjusted to 5.0 by dilute  $\text{HNO}_3$  and  $(\text{CH}_2\text{OH})_3\text{CNH}_2$ . All of the required materials for coating purchased from Merck. Deposition was performed with fixed frequency of 100 Hz by pulse peak current densities of 40mA.cm<sup>-2</sup>, positive pulse duty cycles of 0.1 and temperature of 85°C. The duty cycle ( $\gamma$ ) corresponds to the percentage of total time of a cycle and is given by Equation (1) [10]:

$$\text{Duty cycle } (\gamma) = t_{\text{on}} / (t_{\text{on}} + t_{\text{off}}) \quad (1)$$

$t_{\text{on}}$  is time of applied pulse potential and  $t_{\text{off}}$  is time of no current/ potential. The positive plating time was 10ms

and the deposition process lasted for 0.5h. When the specimens were coated with calcium phosphate, they were removed from the electrolyte solution, rinsed in distilled water and dried for about 4h in air. Then, the as-deposited samples were immersed in 0.25mol.L<sup>-1</sup> NaOH solution at 80°C for 4h, rinsed in distilled water and dried at 80°C for 4h.

**2.3. Coating Characterization** Chemical composition of the coatings was performed by X-ray diffractometer (Philips 1800PW) with  $\text{Cu K}_\alpha$  radiation. The surface morphology and element composition of the coatings were identified by scanning electron microscopy (Tscan-Vega) equipped with energy dispersion spectroscopy facility.

**2. 4. Electrochemical Measurement** The potentiodynamic polarization curves were obtained using a potentiostat (Autolab/PGSTAT302N) at a constant voltage scan rate of 5mv.s<sup>-1</sup>. Experiments were carried out in SBF at 37°C. A three-electrode cell with the samples as the working electrodes was used for the electrochemical measurements. The reference electrode was an Ag–AgCl electrode and the counter electrode was made of platinum. The area of the working electrode exposed to the solution was 0.85cm<sup>2</sup>. The composition and preparation procedure of SBF were as reported in Ref. [15]. The solution was buffered at pH of 7.4 using tris-hydroxymethyl aminomethane ( $(\text{HOCH}_2)_3\text{CNH}_2$ ) and HCl at 37°C. Each result was taken as the mean value of testing on five samples.

## 3. RESULTS AND DISCUSSIONS

### 3. 1. Microstructure and Composition of Scaffold

The optical and SEM micrographs of porous Mg-3Zn (wt.%) scaffold is shown in Figures 1 and 2, where the porosity of the specimen is  $\approx 23$  vol. % using Ref. [1].

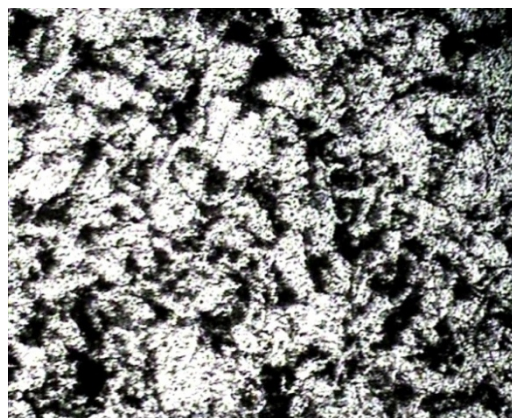


Figure 1. Optical micrograph of the Mg-3Zn (wt.%) scaffold.

The black phases belong to porosity and bright phases correspond to matrix. Some pores were interconnected and the porous magnesium-zinc had an open-cell structure. However, there were isolated pores which were not interconnected and formed as a result of volume shrinkage of the powders during the sintering process. EDS analysis of point A (Figure 2) is shown in Figure 3. As observed in the pattern, the sintered scaffold contains Mg and Zn elements.

### 3. 2. Microstructure and Composition of Coating

Figures 4 and 5 show the X-ray diffractometer (XRD) patterns of the as-deposited and post-treated coatings on porous Mg-3Zn (wt.%) scaffolds. During electrodeposition process a mixture of  $\text{Ca}_{10}(\text{PO}_4)_6(\text{OH})_2$  (HA),  $\text{CaHPO}_4 \cdot 2\text{H}_2\text{O}$  (DCPD) and  $\text{Ca}_8\text{H}_2(\text{PO}_4)_6 \cdot 5\text{H}_2\text{O}$  (OCP) was formed (as-deposited coating). In fact, with applying a high cathode current, the cathodic polarization of the Magnesium alloy leads to an increase in the pH at the interface between the alloy and the electrolyte. Not only does this sudden increase in pH trigger crystal nucleation of the desired Ca-P phase directly on the scaffold surface, but also that initiates the Ca-P crystal growth. The electrodeposition reactions on the surface of scaffold are reduction reaction of  $\text{H}_2\text{PO}_4^-$  and  $\text{HPO}_4^{2-}$  and reaction of  $\text{Ca}^{2+}$  with  $\text{PO}_4^{3-}$ ,  $\text{OH}^-$  and  $\text{HPO}_4^{2-}$  to form HA, DCPD and OCP. DCPD and OCP formed on the as-deposited coating are changed into HA after alkali treatment with NaOH solution.

Figures 6 and 7 show SEM micrographs of the as-deposited and post-treated coatings. The as-deposited and post-treated coatings have needle-like morphology less than 100nm in diameter. However, the as-deposited coating shows some plate-like structures less than 100nm in thickness.

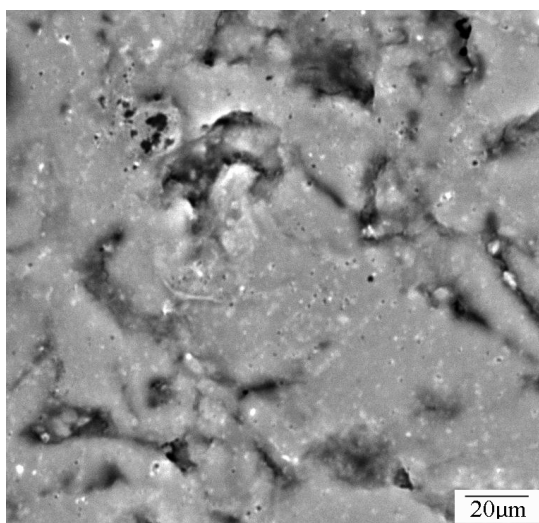


Figure 2. SEM micrograph of the Mg-3Zn (wt.%) scaffold.

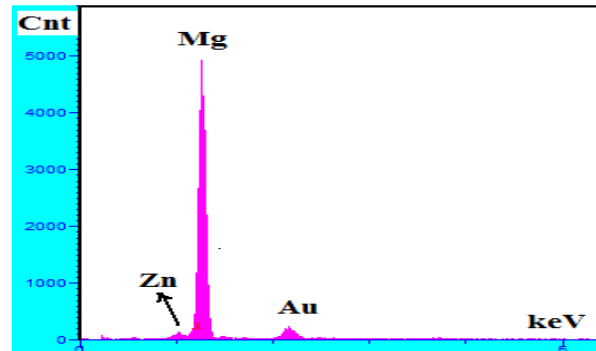


Figure 3. EDS analysis of the Mg-3Zn (wt.%) scaffold.

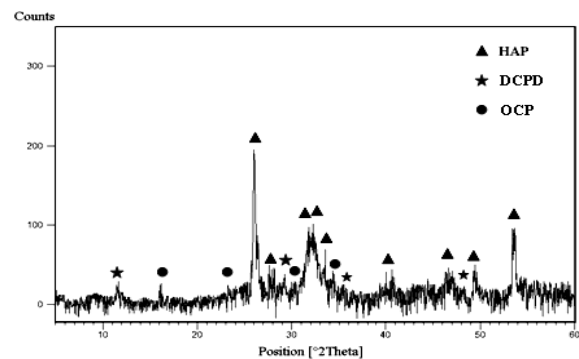


Figure 4. XRD pattern of as-deposited coatings.

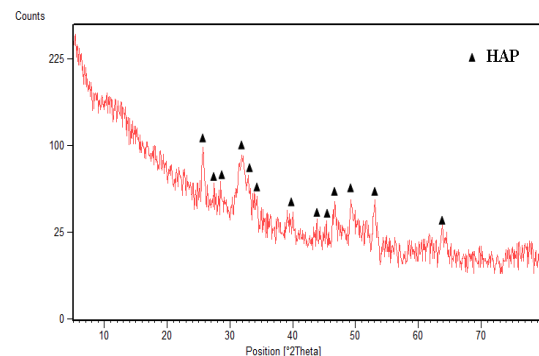


Figure 5. XRD pattern of post-treated coatings by NaOH.

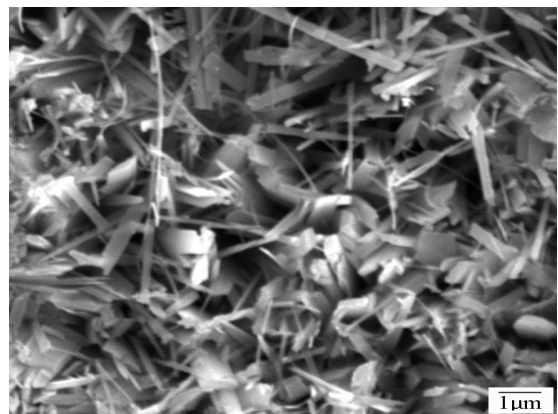


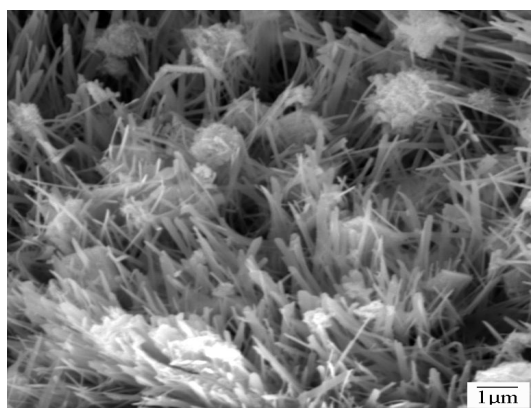
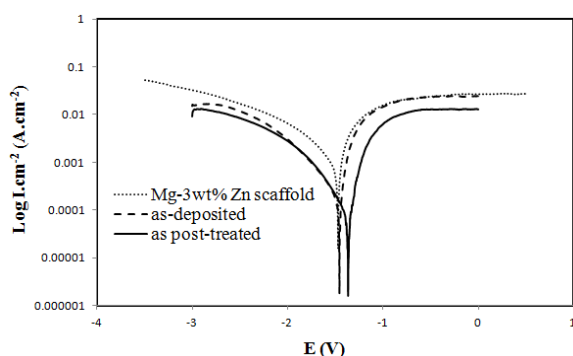
Figure 6. SEM micrograph of as-deposited coating.

**TABLE 1.** EDS analysis of as-deposited coating

Element	At. %
O k	73.07
Na k	3.1
P k	9.45
Ca K	14.38

**TABLE 2.** EDS analysis post-treated coating by NaOH

Element	At. %
O k	66.59
P k	13.96
Ca K	19.45

**Figure 7.** SEM micrograph of post-treated coating by NaOH**Figure 8.** Polarization curves of Mg-3Zn (wt.%) scaffold, as-deposited and post-treated HA-coated specimens in SBF

This structure difference could be attributed to a small amount of DCPD and OCP contained in the as-deposited coating. The needle-like structure might provide more area for the deposition of Ca and P in SBF compared to plate-like surface. In addition, in the post-treated coating, these needles are developed almost

perpendicular to the substrate. It may be beneficial to have a needle-like structure for bone growth [9]. Energy dispersion spectroscopy (EDS) analysis in Tables 1 and 2 show that the coatings contain Ca, P, O, Mg and Na. The  $Mg^{2+}$  and  $Na^+$  ions may substitute the  $Ca^{2+}$  position [4, 9]. It is found that Ca/P atomic ratio is always improved to a certain extent after post-treating by NaOH due to DCPD and OCP having converted to HA. The average Ca/P atomic ratios of the as-deposited and post-treated are calculated at about 1.39 and 1.52, respectively. Those are both lower than the theoretical value of 1.67 for HA. Therefore, the prepared coating is Ca-deficient HA (CDHA, Ca-P with an atomic ratio ranging 1.33-1.65). Many studies have indicated that the dissolution of HA in the human body after implantation is too slow to achieve optimal results, while Ca-def HA seems to be more soluble and may induce precipitation of a new bonelike apatite after. Thus, this just meets the requirements for biodegradable scaffolds [9].

### 3. 2. Electrochemical Behavior of Samples

Electrochemical polarization curves for different samples in SBF are shown in Figure 8. The anodic polarization curves show a passivation-like region indicating the existence of a protective film on the surface of scaffold. In fact, as Kannan and Raman [16] reported, phosphate and calcium ions in SBF could precipitate on the surface of magnesium and, thus, a protective film will form on the surface. Values of corrosion potential ( $E_{corr}$ ), corrosion current density ( $i_{corr}$ ), cathodic and anodic tafel slopes are listed in Table 3 and 4. The  $E_{corr}$  of substrate significantly increased from -1.475 to -1.365V after surface modification by HA. According to the data,  $i_{corr}$  of Mg-3Zn (wt.%) scaffold reduced from  $7.6 \times 10^{-3}$  to  $1.1 \times 10^{-4}$  A.cm<sup>-2</sup> which means HA coating has increased the corrosion resistance of the scaffold in the SBF.

**TABLE 3.** Electrochemical Parameters of the Scaffolds Obtained from The Polarization Curves.

Specimen	$E_{corr}$ (V)	$i_{corr}$ (A.cm <sup>-2</sup> )
Mg-3wt%Zn scaffold	-1.475	$7.6 \times 10^{-3}$
as-deposited HA-coated	-1.455	$1.05 \times 10^{-3}$
post-treated HA-coated	-1.365	$1.1 \times 10^{-4}$

**TABLE 4.** Amounts of Cathodic and Anodic Tafel Slopes of the Scaffolds Obtained from The Polarization Curves.

Specimen	$\beta_c$ (V.dec <sup>-1</sup> )	$\beta_a$ (V.dec <sup>-1</sup> )
Mg-3wt%Zn scaffold	1.265	0.492
as-deposited HA-coated	1.172	0.364
post-treated HA-coated	0.965	0.351

In fact, the formed HA coating protects scaffold from environmental attacks. It could be seen that  $E_{\text{corr}}$  and  $i_{\text{corr}}$  changed, respectively, from -1.455 to -1.365V and from  $1.05 \times 10^{-3}$  to  $1.1 \times 10^{-4}$  A.cm<sup>-2</sup> after alkali treatment. Thus, it is concluded that the alkali treatment can increase the scaffold corrosion resistance. These phenomena indicate that the alkali treatment causes the HA coating to have a better stability. Therefore, not only does the protection capacity of the substrate depend on the chemical composition of the coating, but also it depends on the coating's stability.

#### 4. CONCLUSION

Nano hydroxyapatite coating with needle-like morphology was formed by pulse electrodeposition method to improve the biodegradation behavior of porous Mg-3Zn (wt.%) scaffold. The as-deposited coating containing calcium phosphates such as HAP, DCPD and OCP exhibited mainly needle-like and partially plate-like structures. After alkali treatment, the post-treated coating presented needle-like HA particles of less than 100nm in diameter. The  $E_{\text{corr}}$  value of the Mg-3Zn (wt.%) scaffold increased from -1.475 to -1.365V and  $i_{\text{corr}}$  reduced from  $7.6 \times 10^{-3}$  to  $1.1 \times 10^{-4}$  A.cm<sup>-2</sup> after surface modified by HA coatings. This study revealed that the Ca-def HA coating can therefore effectively reduce the corrosion of the Mg scaffold in SBF.

#### 5. REFERENCES

- Zhuang, H., Han, Y. and Feng, A., "Preparation, mechanical properties and in vitro biodegradation of porous magnesium scaffolds", *Materials Science and Engineering: C*, Vol. 28, No. 8, (2008), 1462-1466.
- Wen, C., Mabuchi, M., Yamada, Y., Shimojima, K., Chino, Y. and Asahina, T., "Processing of biocompatible porous Ti and Mg", *Scripta Materialia*, Vol. 45, No. 10, (2001), 1147-1153.
- Atrens, A., Liu, M. and Zainal Abidin, N.I., "Corrosion mechanism applicable to biodegradable magnesium implants", *Materials Science and Engineering: B*, Vol. 176, No. 20, (2011), 1609-1636.
- Wen, C., Guan, S., Peng, L., Ren, C., Wang, X. and Hu, Z., "Characterization and degradation behavior of AZ31 alloy surface modified by bone-like hydroxyapatite for implant applications", *Applied Surface Science*, Vol. 255, No. 13, (2009), 6433-6438.
- Gu, X., Zheng, Y., Zhong, S., Xi, T., Wang, J. and Wang, W., "Corrosion of, and cellular responses to Mg-Zn-Ca bulk metallic glasses", *Biomaterials*, Vol. 31, No. 6, (2010), 1093-1103.
- Kaya, A., Eliezer, D., Ben-Hamu, G., Golan, O., Na, Y. and Shin, K., "Microstructure and corrosion resistance of alloys of the Mg-Zn-Ag system", *Metal Science and Heat Treatment*, Vol. 48, No. 11-12, (2006), 524-530.
- Yin, D.-S., Zhang, E.-L. and Zeng, S.-Y., "Effect of Zn on mechanical property and corrosion property of extruded Mg-Zn-Mn alloy", *Transactions of Nonferrous Metals Society of China*, Vol. 18, No. 4, (2008), 763-768.
- Zhang, E., Yin, D., Xu, L., Yang, L. and Yang, K., "Microstructure, mechanical and corrosion properties and biocompatibility of Mg-Zn-Mn alloys for biomedical application", *Materials Science and Engineering: C*, Vol. 29, No. 3, (2009), 987-993.
- Wang, H., Guan, S., Wang, X., Ren, C. and Wang, L., "In vitro degradation and mechanical integrity of Mg-Zn-Ca alloy coated with Ca-deficient hydroxyapatite by the pulse electrodeposition process", *Acta Biomaterialia*, Vol. 6, No. 5, (2010), 1743-1748.
- Saremi, M. and Motaghi Golshan, B., "Electrodeposition of nano size hydroxyapatite coating on Ti alloy", *Iranian Journal of Materials Science and Engineering*, Vol. 3, No. 3, (2006), 1-5.
- Song, Y., Shan, D. and Han, E., "Electrodeposition of hydroxyapatite coating on az91d magnesium alloy for biomaterial application", *Materials Letters*, Vol. 62, No. 17, (2008), 3276-3279.
- Li, W., Guan, S., Chen, J., Hu, J., Chen, S., Wang, L. and Zhu, S., "Preparation and in vitro degradation of the composite coating with high adhesion strength on biodegradable mg-zn-ca alloy", *Materials Characterization*, Vol. 62, No. 12, (2011), 1158-1165.
- Chun-Yan, Z., Rong-Chang, Z., Cheng-Long, L. and Jia-Cheng, G., "Comparison of calcium phosphate coatings on Mg-Al and Mg-Ca alloys and their corrosion behavior in Hank's solution", *Surface and Coatings Technology*, Vol. 204, No. 21, (2010), 3636-3640.
- Meng, E., Guan, S., Wang, H., Wang, L., Zhu, S., Hu, J., Ren, C., Gao, J. and Feng, Y., "Effect of electrodeposition modes on surface characteristics and corrosion properties of fluorine-doped hydroxyapatite coatings on Mg-Zn-Ca alloy", *Applied Surface Science*, Vol. 257, No. 11, (2011), 4811-4816.
- Kokubo, T. and Takadama, H., "How useful is SBF in predicting in vivo bone bioactivity?", *Biomaterials*, Vol. 27, No. 15, (2006), 2907-2915.
- Kannan, M.B. and Raman, R., "In vitro degradation and mechanical integrity of calcium-containing magnesium alloys in modified-simulated body fluid", *Biomaterials*, Vol. 29, No. 15, (2008), 2306-2314.

# Electrodeposition of Nano Hydroxyapatite Coating on Biodegradable Mg-Zn Scaffold

TECHNICAL  
NOTE

Z. S. Seyedraoufi, S. Mirdamadi, S. Rastegari

Center of Excellence for High Strength Alloys Technology ( CEHSAT), School of Metallurgy and Materials Engineering, Iran University of Science and Technology, 16846-13114, Tehran, Iran

## PAPER INFO

چکیده

### Paper history:

Received 11 September 2013

Received in revised form 17 October 2013

Accepted 12 December 2013

### Keywords:

Biodegradable Mg-Zn Scaffold

Nano Hydroxyapatite Coating

Electrodeposition

Corrosion Resistance

در این تحقیق، داربست‌های منیزیم-روی متخلخل از طریق فرایند متالورژی پودر آماده شدند و پوشش نانو هیدروکسی آپاتیت بر روی داربست منیزیمی حاوی ۳ درصد وزنی عنصر روی توسط فرآیندهای رسوب الکتریکی پالسی و عملیات قلیایی جهت بهبود مقاومت خوردگی داربست ایجاد شد. نتایج نشان داد که پوشش حاصل از فرایند رسوب الکتریکی پالسی شامل HAP با ساختار سوزن‌مانند و مقداری نیز شامل ترکیبات OCP و DCPD با ساختار صفحه‌مانند می‌باشد. پوشش حاصل از عملیات قلیایی نیز از ذرات سوزنی HAP تقریباً عمود بر زیرپایه تشکیل شده بود. آزمون‌های الکتروشیمیایی نشان داد که پتانسیل خوردگی داربست به طور قابل توجهی از  $-1/475$  به  $-1/365$  ولت افزایش و چگالی جریان خوردگی در حدود یک و نیم برابر در مقایسه با داربست اصلاح شده توسط پوشش نانو هیدروکسی آپاتیت کاهش یافت.

doi: 10.5829/idosi.ije.2014.27.06c.12